Multicomponent Prestack Modeling in Isotropic/Anisotropic Media

Jim Simmons, GX Technology

2004 CSEG National Convention

Introduction

Nine-component (9-C) 3-D seismic reflection data are acquired using vertical and two orthogonal shear-wave vibrators as seismic sources, and three-component (3-C) geophones. Shear-wave sources are usually oriented inline and crossline to the receiver cables, as are the horizontal geophone components. Three-component (3-C) geophones record the ground particle motion for each of the three sources over an areal grid in (x,y).

Conventional 3-C data include the x, y, and z particle motions (R_x, R_y, and R_z, respectively) recorded from a vertical vibrator (S_z) or explosive source (E). Conventional P-wave data are taken as the R_z component, while C-wave data are taken as the R_x and R_y components. Horizontal receiver-components R_x and R_y are then rotated into a radial-transverse (R,T) coordinate system (R_R and R_T) for C-wave processing and analysis. Rotation from (x,y) to (R,T) coordinates removes the dependence on source-receiver azimuth inherent to 3-D shooting geometries. C-wave processing and analysis then emphasizes the radial receiver component R_R, while nonzero R_T is used as an indicator of shear-wave splitting.

Four shear-wave datasets result from 9-C acquisition (S_x,R_x; S_x,R_y; S_y,R_x; S_y,R_y), where S_x and S_y are horizontal forces (horizontal vibrators) oriented in the x and y directions. Horizontal receiver components are also oriented in the x and y directions. Note that the S_x,R_z and S_y,R_z components are neglected. Historically, these shear-wave datasets have been processed independently to varying degrees, with coherent energy on the crossterms (S_x,R_y and S_y,R_x) diagnostic of shear-wave splitting. It is also common to rotate into a coordinate system that is parallel and perpendicular to a predetermined maximum horizontal stress direction, say (x',y') where crossterms $S_{x'}$,$R_{y'}$ and $S_{y'}$,$R_{x'}$ are now indicative of shear-wave splitting.

There seems to be a general lack of multicomponent prestack forward modeling to: :validate C-wave and S-wave processing methodologies, validate interpretations with regard to shear-wave splitting and fractured reservoirs, evaluate amplitude-versus-offset-azimuth analysis of P-waves, C-waves, and S-waves, and to quantify the sensitivity of multicomponent data to various fractured-reservoir models.

Full-waveform reflectivity modeling simulates prestack multicomponent data for a 1-D earth model (earth properties vary only with depth) where any/all layers may be arbitrarily anisotropic (21 elastic stiffnesses, C_{ij}). The prestack modeling is 3-D in that seismic traces are calculated over an areal, and equally sampled, grid in (x,y), for seismic sources located at the center of the grid. As a result, wide-azimuth and wide-offset 3-C, 9-C, or 4-C data may be simulated in isotropic/anisotropic media. Since the acquisition geometry is 3-D, the directivity of the seismic sources (S_x, S_y, S_z, and E) is incorporated.

I simulate 9-C 3-D prestack data from relatively simple isotropic, and anisotropic models to illustrate the effects of source-receiver azimuth and source type on the 3-C data recorded at any (x,y) location. Data recorded from shear-wave sources are especially interesting due to the directivity of the horizontal-force sources. Significant crossterm energy is present on shear-wave components, S_x,R_y; S_y,R_x in an *isotropic earth* because of variable source-receiver azimuth inherent to 3-D acquisition. Rotation to radial-transverse coordinates is necessary for the shear-wave source data to remove crossterm energy produced by source-receiver azimuth, focus SV and SH data onto single data components, and expose any shear-wave splitting that may exist.

Reflectivity modeling: Earth model and seismic system

The earth model consists of horizontal, homogeneous layers where any or all layers may be generally anisotropic (21 C_{ij}'s). Three-component geophones are equally spaced in x and y over a square grid from $-x_{\max} \le x \le x_{\max}$, and $-y_{\max} \le y \le y_{\max}$, at a constant receiver depth. Seismic sources are located at x=0, y=0, and may be forces oriented along the x-, y-, and z-coordinate axes (i.e. orthogonal horizontal vibrators and a vertical vibrator, respectively), and/or an explosion. Source directivity is accurately modeled as will be seen in the synthetic examples.

Three-dimensional 3-C prestack data cubes are generated for each specified source. Plane waves are propagated through the layered stack for all temporal frequencies ω, and positive and negative horizontal wavenumbers k_x and k_y. Negative wavenumbers are needed to properly simulate shot-receiver azimuth effects, properly model source directivity, and to generate the seismic response in anisotropic media (Fryer and Frazer, 1984; 1987). Kennett's recursion relations (Kennett, 1983) are used to propagate the reflection-transmission coefficients downward through the layered medium, and to calculate the complete plane-wave response, $U(\omega,k_x,k_y)$, for each source type. Since $U(\omega,k_x,k_y)$ is equally sampled in (ω,k_x,k_y), a 3-D inverse Fourier Transform produces the 3-C prestack data in the time-space domain as. d(t,x,y).

All wavemodes are generated by the reflectivity modeling; primary reflections (P-P, SV-SV, SH-SH), converted waves (P-SV, SV-P), head waves, all interbed multiples, as well as surface multiples and surface waves depending on whether free surface effects are included. Free surface effects are not included in any of the model simulations shown here.

Isotropic model: Source-receiver azimuth, SV and SH

Two isotropic elastic layers are embedded within an isotropic full space (i.e., no free surface effects) resulting in three reflecting interfaces with which to illustrate the multicomponent reflectivity modeling. The earth model is the isotropic model of Shen et al., 2002). Sources and receivers are located at the same depth. Full 3-D modeling simulations produce prestack data cubes for force sources oriented in the +x, and +y directions (S_x, and S_y, , respectively). Three-component data recorded along the x-axis (y=0) and along the y-axis (x=0) are shown for sources S_x and S_y in Figures 1 and 2, respectively. A cube icon at the upper right of each subpanel shows the orientation of the receiver line relative to the 3-D acquisition over which data are generated. The location of the seismic sources is at the center of the cube as shown.

Data recorded along the y=0 axis (source-receiver azimuth, ϕ = 0) for source S_x are equivalent to data obtained from a 2-D SV seismic experiment (Figure 1,top). Receiver component R_y=0, since the receiver component is perpendicular to the particle motion generated by the source, the earth model is isotropic, and ϕ = 0. SV data would be taken as the S_x,R_x component. Note that at ϕ=0, the horizontal force generates a direct P-wave arrival seen on R_x but not on R_z , since the particle motion is in the x-direction. P-waves are generated by the horizontal force, apparent from the P-P and P-S reflection events. R_z is neglected in conventional S-wave and C-wave data analysis.

Orientation of the receiver profile along the x=0 axis (ϕ = 90 degrees) now produces SH data recorded on the R_x receiver component. A strong SH direct arrival is apparent, as are SH-SH reflections. Receiver component R_y and R_z are zero at this source-receiver azimuth since all particle motion is in the x direction. Note that for the same source and same receiver component (S_x,R_x), pure SV data are recorded when ϕ =0, and pure SH data are recorded when ϕ=90. This is important to note since conventional 9-C 3-D shear-wave data analysis would take S_x,R_x as a shear-wave dataset to be further processed and analyzed. It is most apparent from this figure that SV and SH data are indeed very different, and are best treated as such. Note the obvious differences between SV reflections (top) and SH reflections (bottom) on S_x,R_x.

Analogous displays for the S_y source (horizontal force oriented along the x=0 axis) are shown in Figure 2. At ϕ=0, pure SH data are recorded on R_y, with R_x=0 and R_z=0, since the receiver profile is oriented perpendicular to the particle motion. At ϕ=90, the SV data are recorded on R_y and R_z, and R_x=0 since all particle motion is in the y-z plane which is parallel to the receiver profile.

Clearly, source-receiver azimuth controls the types of wavemodes recorded on a given source-receiver combination (S_x, R_x; S_y,R_y, etc.) in a simple isotropic earth. Receiver profiles oriented parallel and perpendicular to the source motion (Figures 1 and 2) may be considered as the end members in that the crossterm (receiver component perpendicular to the source motion (R_y for S_x, R_x for S_y) is zero. Prestack time slices through the data cube, d(t_{fixed},x,y), show the rotation of the (x,y,z) particle motion as ϕ varies from 0 to 90 degrees. The crossterms reach maximum amplitude at ϕ=45 degrees due solely to source-receiver azimuth. An example of nonzero crossterms in an isotropic model is shown later in Figure 4.

Radial-transverse coordinates

Three-component C-wave and VSP data are rotated to (R,T) coordinates to remove the ϕ dependence and focus the horizontal component of particle motion onto the radial receiver component, R_R. The transverse receiver component, R_T, is then used as an indicator of shear-wave splitting. It is interesting, and most curious, that the shear-wave source data are not analyzed in (R,T) coordinates. As a result, the variable source-receiver azimuth inherent to 3-D acquisition geometries produces nonzero crossterms even for an isotropic earth when the data are processed/analyzed in field (x,y) coordinates. The variable source-receiver azimuth produces SV (and P) wave data along preferred azimuths on both S_x,R_x and S_y,R_y data, produces SH waves at other azimuths as seen in Figures 1 and 2, and a mixture of SV, P, and SH waves (and nonzero $S_{x'}$,$R_{y'}$ and $S_{y'}$,R_x!) at all other azimuths (which will be seen in Figure 4).

Rotation of the shear-wave source data (S_x,R_x; S_x,R_y:S_y,R_x;S_y,R_y) to a radial-transverse (R,T) coordinate system (S_R,R_R; S_R,R_T; S_T,R_R; S_T,R_T) removes the source-receiver azimuth dependence just as it does for 3-C data (surface and borehole). Each prestack trace is oriented into a radial-transverse coordinate system with the rotation angle determined by the (x,y) location of source and receiver.

SV and SH data taken from the respective source-receiver combinations (from Figures 1 and 2) are shown with the radial-transverse data, S_R,R_R and S_T,R_T, in Figure 3. Components S_R,R_T and S_T,R_R,are zero and not shown. In field (x,y) coordinates, S_x,R_x contains SV data at ϕ=0, and SH data at ϕ=90. Similarly, S_y,R_y contains SH data at ϕ=0, and SV data at ϕ=90. After rotation to a radial-transverse coordinate system, S_R,R_R contains SV data at all azimuths, and S_T,R_T contains SH data at all azimuths.

Data recorded along a receiver profile that is offset in the +y direction from the source location is shown in Figure 4. Since the source-receiver azimuth is variable along the receiver profile, energy is recorded on all data components. Note the large amplitude of the crossterms (S_x,R_y and S_y,R_x) for an isotropic model. Consequently, each data component contains a mixture of SH, SV, and P-waves, with pure SV and pure SH data being recorded only at lateral offset (in x) =0 since this offset corresponds to ϕ=-90. Meanwhile, the radial-transverse data (Figure 4, lower) show focusing of the SV data on S_R,R_R, focusing of SH data on S_T,R_T, with zero crossterm energy.

Anisotropy: HTI model

The importance of removing the effect of source-receiver azimuth to expose shear-wave splitting effects is shown in Figures 5 and 6**.** The earth model is that of an oil-filled carbonate layer containing vertical fractures (HTI layer) overlain by a thick isotropic layer (Shen et al., 2002). The strike of the vertical fractures (fast direction) is at an angle of 30 degrees relative to the x-axis. Field coordinate shear-wave data are shown in Figure 5 with for receiver profiles along the x- and y-axes. Similar to the isotropic example, at ϕ=0 S_x,R_x is dominantly SV and S_Y,R_Y is dominantly SH. Note that there is some polarization of energy onto the crossterms produced by shear-wave splitting. The amount of shear-wave splitting at normal incidence is roughly 8 ms. Only the energy that propagates though the fractured layer, or reflects from the top of the fractured layer, appears on the crossterms, S_R,R_T and S_T,R_R. At ϕ=90, S_X,R_X contains predominantly SH data, and S_Y,R_Y contains predominantly SV data.

The magnitude of the source-receiver azimuthal effect relative to the magnitude of the shear-wave splitting effect is revealed when examining the data recorded at a nonzero y offset (Figure 6). Shear-wave splitting cannot be inferred from the (x-y) data due to the dominance and variability of source directivity and source-receiver azimuth. Rotation to radial-transverse coordinates exposes the shear-wave splitting on the crossterms, S_R,R_T and S_T,R_R.

C-wave and shear-wave azimuth stacks for the HTI model are shown in Figures 7 and 8, respectively. C-wave data are obtained from the vertical-force source (S_Z), and azimuth stacks are created by applying t^2 gain, NMO correction, and stacking the data within 10-degree azimuth bins. The transverse component is minimum and changes polarity at the preferred orientations (ϑ=30 +/- 90 degrees), while the radial component shows variation in amplitude with azimuth from the top and base fractured-reservoir reflections, and a sinusoidal oscillation in traveltime for the base-reservoir reflection. Fast directions are at azimuths of 30 and 210 degrees, and the slow directions are at 120 and 300 degrees.

The shear-wave source azimuth stacks (Figure 8) show similar features, albeit with increased sensitivity since both the incident and reflected shear-waves are affected by the fractures. Note that S_R,R_R is parallel to the fractures (fast) at 30 degrees, while S_T,R_T is perpendicular to the fractures (slow). At 120 degrees, the situation reverses: S_R,R_R is slow and S_T,R_T is fast. Also note that the conventional terminology for fast and slow shear waves, S_1 and S_2, respectively, now becomes somewhat confused in that S_R,R_R (essentially SV) has a fast and slow direction as does S_T,R_T (essentially SH).

Summary

Prestack modeling of multicomponent data in isotropic/anisotropic media will prove valuable in validating multicomponent processing and interpretation methodologies. The importance of treating 9-C shear-wave source data similarly to C-wave data in radial-transverse coordinates is critical to expose shear-wave splitting effects that may be present in the data.

References

Fryer, G.J., and Frazer, L.N., 1984, Seismic waves in stratified anisotropic media: Geophys. J. Royal Astron. Soc, **78**, 691-710.

Fryer, G.J., and Frazer, L.N., 1984, Seismic waves in stratified anisotropic media-II. Elastodynamic eigensolutions for some anisotropic systems: Geophys. J. Royal Astron. Soc, **91**, 73-101

Kennett, B.L.N., 1983, *Seismic wave propagation in stratified media*: Cambridge University Press, p. 342.

Shen, F., Sierra, J., Burns, D.R., and Toksoz, M.N., 2002, Azimuthal offset-dependent attributes applied to fracture detection in a carbonate reservoir: Geophysics, **67**, 355-364.

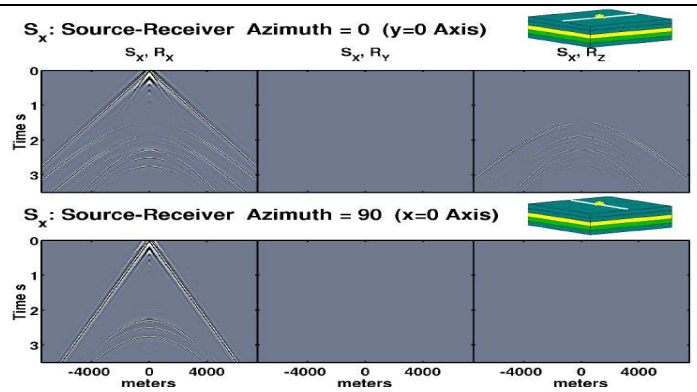

Figure 1: X-force source, 3-C data recorded along the receiver profiles indicated; y=0 axis (top), x=0 axis (bottom), isotropic model.

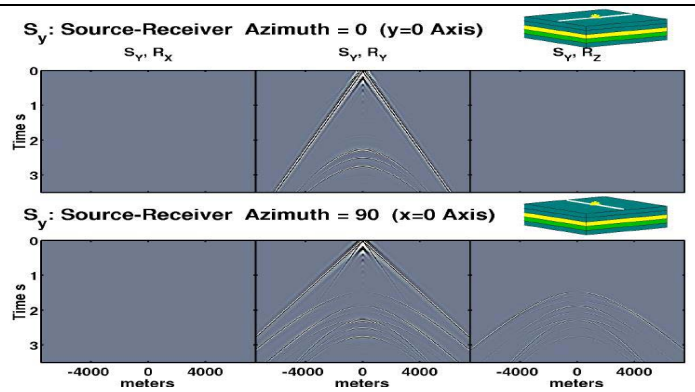

Figure 2: Y-force source, 3-C data recorded along the receiver profiles indicated. Isotropic model.

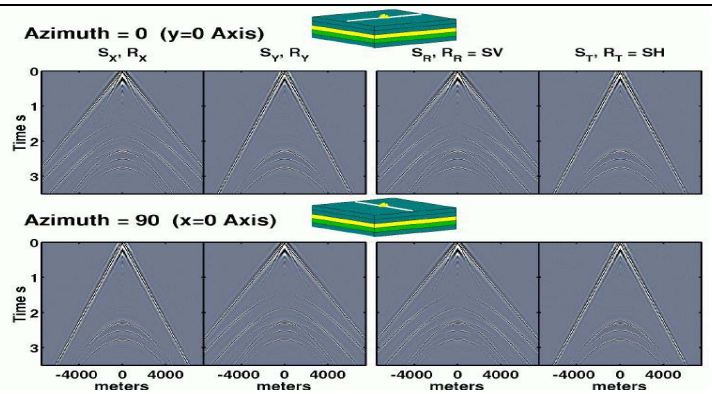

Figure 3: Field coordinate (left) and radial-transverse coordinate (right) 3-C data for the receiver profiles shown. Isotropic model.

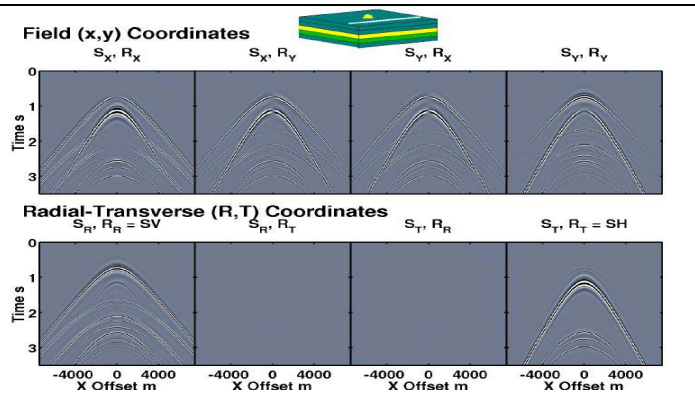

Figure 4: Field coordinate (top) and radial-transverse coordinate (bottom) 3-C data for the receiver profile shown. Isotropic model.

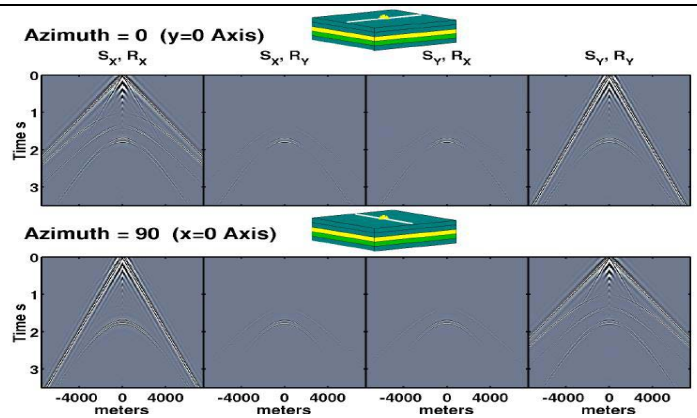

Figure 5: X-force generated 3-C data (S_x) recorded along y=0 (top) and x=0 (bottom) axes for an anisotropic model (HTI reservoir layer).

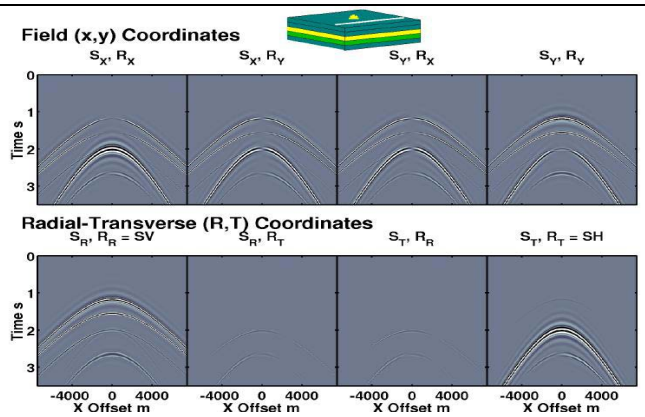

Figure 6: X-force generated 3-C data (S_y) recorded along the y=0 (top) and x=0 (bottom) axes for an anisotropic model (HTI reservoir layer).

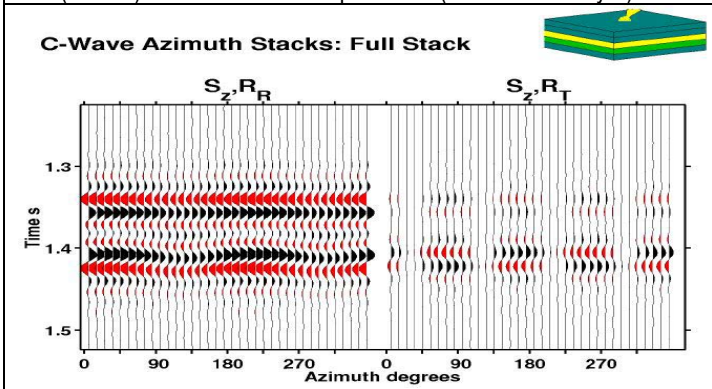

Figure 7: C-wave azimuth stacks, vertical force source, anisotropic model.

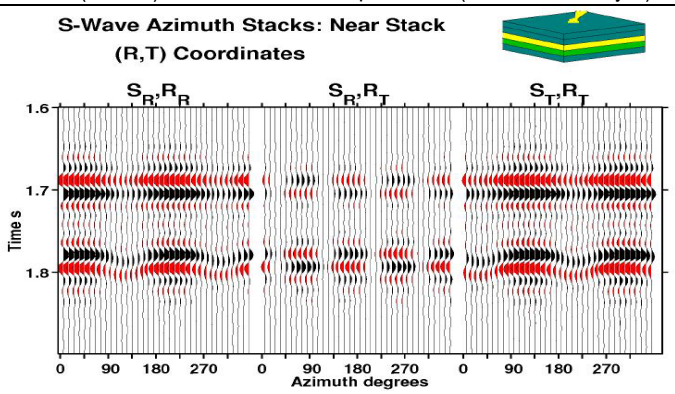

Figure 8: Shear-wave azimuth stacks, radial-transverse coordinates, anisotropic model.